Influence of Source Antenna Beamwidth on Far-Field Measurement Method Using Numerical Compact Range

Ryo Yamaguchi, #Kazuhiro Komiya, Keizo Cho
Research Laboratories, NTT DOCOMO, INC.
3-5 Hikari-no-oka, Yokosuka-shi, Kanagawa 239-8536 Japan
E-mail: komiya@nttdocomo.co.jp

1. Introduction

A cellular base station antenna has a narrow beamwidth in the vertical plane because the length of the antenna is longer than 10 λ. While generally long distance measurements are needed to measure an electrically long antenna with high accuracy, some measurement methods in a short-range anechoic chamber have been used. For this purpose, the compact range method [1-2] and near-far field transformation method [3-6] are very popular. However, since additional hardware, which is large or expensive, is needed to employ these methods, it is difficult to measure the far-field pattern of an antenna compared to using conventional pattern measurement methods in an anechoic chamber.

In order to overcome this problem, a far-field measurement method was proposed for electrically long antennas using a conventional pattern measurement system when the measurement distance is not sufficient in an anechoic chamber [7]. Since the employed source antenna is treated as a numerical compact range in this method, a virtual quasi-plane wave is generated around the antenna under test (AUT) to obtain the far-field pattern. We clarified the validity of the proposed method that the far-field can easily be obtained in a short range anechoic chamber without extra equipment.

Although the half-power beamwidth of the source antenna is treated as isotropic [7], in this paper, which further investigates the proposed method, the influence of the beamwidth is shown in order to clarify the condition for the source antenna.

2. Measurement Using Numerical Compact Range Concept

The proposed measurement method obtains the far-field radiation pattern by generating a quasi-plane wave around the AUT when it is receiving a signal as shown in Fig. 1. The method can be basically thought of as having a compact range and employing a virtual synthetic aperture array antenna. However, compared to other compact range methods, the range in this method differs in that the scanning track of the virtual synthetic aperture antenna is not a parabola but a circular arc, and the quasi-plane wave can be generated numerically. The proposed method can be generally categorized as a plane-wave synthesis method [5]. It comprises the following two procedures.

1) Actual Measurement in Near-Field

Figure 1 shows the principle of the proposed method. When the AUT is rotated by θ_i, the received electric field, $E_{near}(\theta_i)$, from an actual element at the position of $x=R$ is measured. Complex data (the amplitude and the phase of the field) are required to employ the vector network analyzer. Because the measurement distance, R, is not sufficiently long, the pattern obtained from the raw measurement data is distorted. In this method, however, a numerical compact range can be formed using the distorted measurement data.

2) Plane-Wave Synthesis Using Numerical Compact Range

Virtual elements are symmetrically arranged on both sides of the actual element. The total number of elements for the numerical compact range is $2N+1$. At this time, the configuration of the compact range is an arc, and the elements are arranged at equal intervals (equal angle step $\Delta\psi$). It is

necessary to weight each element with the phase difference corresponding to distance $R(1\text{-}\cos\psi_j)$ in order to synthesize the plane wave in the region for the AUT (on y-axis) because the virtual scanning track is an arc. The obtained far-field value, E_{far}, can be expressed as the sum of the received electric fields, E_{near}, from all the elements at a finite distance as

$$E_{far}(\theta_i) = \sum_{j=-N}^{N} E_{near}(\theta_i + \phi_j) w_j \exp\{jkR(1-\cos\phi_j)\}\Delta\phi, \quad (1)$$

where $E_{far}(\theta_i)$, $E_{near}(\theta_i+\psi_j)$, w_j, R, ψ_j, and $\Delta\psi$ represent the desired far-field, the measured field from the element at finite distance R, the weight, the measurement distance, the relative angle of the j-th element, and the angle step, respectively. Distance $R(1\text{-}\cos\psi_j)$ represents the distance between each virtual element and the reference plane (x=R).

3. Simulation

3.1 Simulation Conditions and Radiation Patterns

In this section, the characteristics of far-field patterns derived from the proposed method are evaluated when the half-power beamwidth of the source antenna is changed. Figure 1 illustrates the image of the beamwidth. The radiation pattern of the source antenna is treated as a cosine function. The viewing angle is defined as an angle between both edges of the AUT as observed from the center source antenna. Simulation specifications are given in Table 1. The aperture of 14.0 λ for a 28-element dipole array antenna, which is typically used in an outdoor base station, is used to evaluate the AUT. A simulation corresponding to an experiment of limited distance (R=66.7 λ) is performed. The symbol of ∞ shown in Table 1 represents an isotropic source antenna.

Figure 2 shows the far-field pattern when the source antenna beamwidth is changed. The solid line indicates the results using the numerical compact range, and the dashed line represents an array factor calculation as a reference. In this figure, the pattern is normalized at the maximum level of the main lobe since the difference in the pattern shape is investigated. In Figs. 2(a) and 2(b), where the beamwidth is over 30 deg., the far-field pattern of the proposed method is the same as the reference. However, Fig. 2(c) shows that the main lobe is slightly larger and the side lobe levels are decreased against the array factor calculation. Moreover, Fig. 2(d) shows that the far-field pattern obtained using the proposed method is completely different from the reference. The reason for this is considered to be that the wave from the source antenna to the AUT is not uniform when the beamwidth is nearly equal or narrower compared to a 12 deg. viewing angle.

3.2 Dependency of Source Antenna Beamwidth

In this section, the difference in electrical field level between the center and the edge of the AUT and the degradation in the first side lobe level are investigated when the source antenna beamwidth is varied.

Figure 3 indicates the dependency of degradation in electrical field level on the source antenna beamwidth. The solid line presents the degradation in the first side lobe level compared to the array factor pattern. This corresponds to the difference in the first side lobe level of the two patterns showed in Fig. 2. The dashed line in Fig. 3 indicates the degradation in electrical field level from the center compared to that at the edge of the AUT. We find that the degradation in electrical field level at the edge is at the same inclination as that for the first side lobe level. This means that the far-field pattern cannot be formed precisely in proportion to a narrow beamwidth.

Figure 4 illustrates the influence of the normalized source antenna beamwidth on the degradation in the first side lobe level. Here, the parameter is the measurement distance that is proportional to the viewing angle when the AUT length is fixed. The x-axis of the figure is normalized to the ratio of the source antenna beamwidth to the viewing angle. The simulation results show that the degradation in the first side lobe level is increased when the normalized source antenna beamwidth is small. Moreover, we find that more than three times the normalized source antenna beamwidth is required when the degradation in the first side lobe level is below 0.2 dB.

4. Conclusion

The influence of the beamwidth was shown in order to clarify the conditions for the source antenna for the proposed measurement method using a conventional pattern measurement system and numerical compact range to obtain the far-field pattern of an electrically long antenna in a short range anechoic chamber. The simulation results showed that the far-field pattern cannot be formed precisely in proportion to a narrow source antenna beamwidth because of the degradation in the electrical field level at the edge of the AUT. Moreover, we showed that more than three times the normalized source antenna beamwidth is required when the degradation in the first side lobe level is below 0.2 dB.

References

[1] R.C. Johnson, H.A. Ecker, R.A. Moore, "Compact range techniques and measurements," IEEE Trans. Antennas Propagat., vol. AP-17, 5, pp. 568-576, Sept. 1969.

[2] J. McCormick, J. Boyce, J. Sayers, J. Murray, "The impact on measurement accuracy of specifying a compact antenna test range for high power testing," Tu1.3.4, EuCAP2008, Nov. 2008.

[3] D.M. Kernes, "Plane wave scattering matrix theory of antennas and antenna-antenna interactions," J. Res. Natl. Bur. Stand., 80-B, 1, p. 5, Sept. 1975.

[4] A.D. Yaghjian, "An overview of near-field antenna measurements," IEEE Trans. Antennas Propagat., vol. AP-34, pp. 30-45, Jan. 1986.

[5] J.E. Hansen, ed., *Spherical Near-Field Antenna Measurements*, Peregrinus, London, 1988.

[6] H. Bartik, F. Kondapaneni, "Application of displaced beam method on antenna radiation pattern measurement," Tu1.3.5, EuCAP2008, Nov. 2008.

[7] R. Yamaguchi, Y. Kimura, K. Komiya, K. Cho, "A far-field measurement method for large size antenna by using synthetic aperture antenna," Wed-S9M3, EuCAP2009, March 2009.

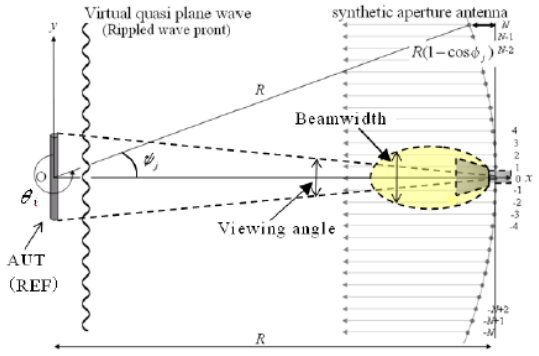

Figure 1: Principle of Proposed Method

Table 1: Simulation Specifications

Frequency	2.0 GHz
Beamwidth of source antenna	5 - 60 deg., ∞
Viewing angle	12 deg.
Number of AUT elements	28
AUT aperture	14.0 λ
Measurement distance	66.7 λ
Synthetic aperture angle	150 deg.
Number of source elements	1501
Angle step	0.1 deg.

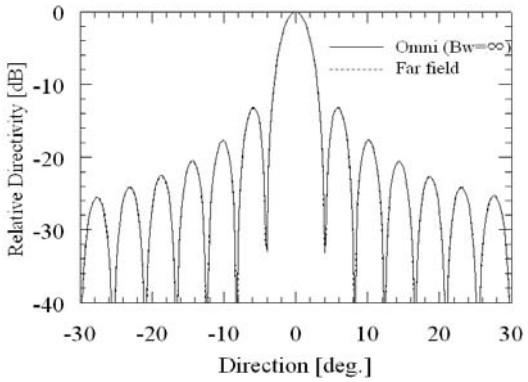

(a) Beamwidth = ∞

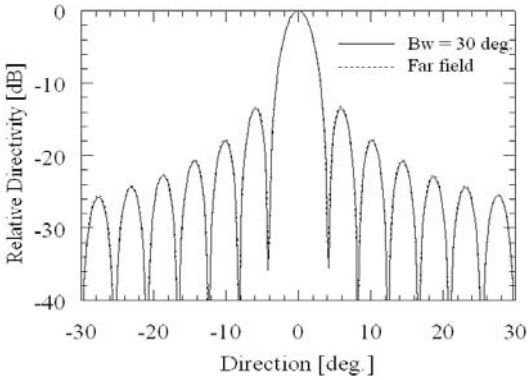

(b) Beamwidth = 30 deg.

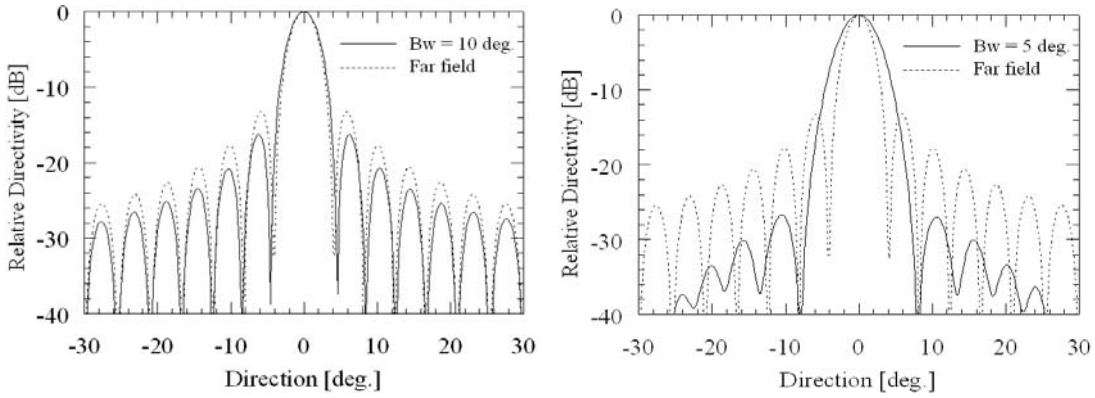

(c) Beamwidth = 10 deg. (d) Beamwidth = 5 deg.

Figure 2: Far-Field Pattern Results

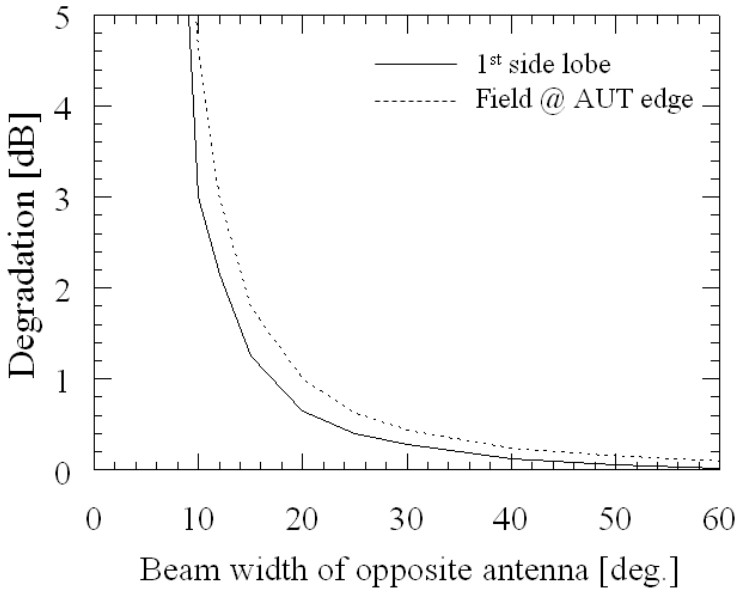

Figure 3: Degradation in Electrical Field Level on Source Antenna Beamwidth

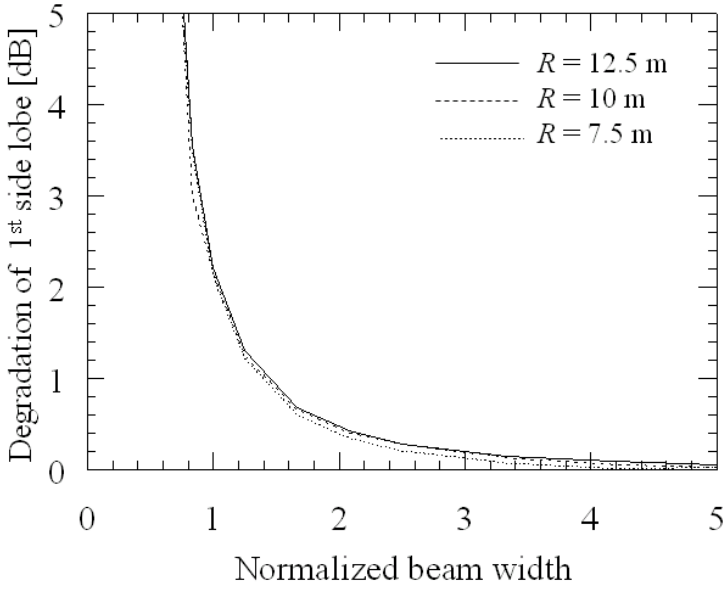

Figure 4: Influence of Normalized Source Antenna Beamwidth